Experimental analysis of cello string types: influence on playability and tonal characteristics using Schelleng diagrams

Alessio Lampis ; Vasileios Chatziioannou ; Gary Scavone

Check for updates

View Online

Export Citation

International Symposium on Music and Room Acoustics

24-28 May 2025

Loyola University
New Orleans, Louisiana

Musical Acoustics

Experimental analysis of cello string types: influence on playability and tonal characteristics using Schelleng diagrams

Alessio Lampis
Department of Music Acoustics (IWK), University of Music and Performing Arts Vienna, Vienna, 1030, AUSTRIA; lampis@mdw.ac.at; alelampis2295@gmail.com

Vasileios Chatziioannou
Department of Music Acoustics – Wiener Klangstil (IWK), University of Music and Performing Arts Vienna: Universitat fur Musik und darstellende Kunst Wien, Wien, 1030, AUSTRIA; chatziioannou@mdw.ac.at

Gary Scavone
McGill University Schulich School of Music, Montreal, QC H3A 1E3, CANADA; gary.scavone@mcgill.ca

This study experimentally assesses the influence of cello string types on playability and tonal characteristics using a robotic bowing device and a custom monochord setup. Eight custom-made G2 cello strings, each defined by unique combinations of core materials, windings, and nominal tensions, were systematically tested. High-resolution Schelleng diagrams were constructed from steady-state signals across various bow forces, bow-bridge distances, and bow speeds. Analyses included bow force limits, spectral centroid, pitch flattening, and anomalous low frequencies. Results revealed similar regions of Helmholtz motion, with deviations from Schelleng's classical theory aligning with recent research. Pitch flattening occurred mainly at high bow forces and lower bow speeds, with deviations up to 60 cents below nominal pitch, while spectral centroid analysis highlighted a significant correlation between bending stiffness and perceived tonal brightness. Minimal within-type variability was noted; however, tonal deviations due to string settling were substantial, underscoring the importance of play-in periods. Although playability differences across tension groups were minor, tonal descriptors, notably spectral centroid, displayed clearer sensitivity to material composition. Future studies should explore broader string variations and detailed harmonic content to enhance statistical robustness and generalizability. This research was funded in whole or in part by the Austrian Science Fund (FWF) [P34852-N].

1. INTRODUCTION

Bowed-string instrument musicians consider a variety of factors when selecting the strings for their instrument. Among these, tone and playability are of particular importance. Although this choice is largely subjective and depends as well on the compatibility with their instruments and their playing style. This raises the question of how the type of string influences sound.

Nowadays, there exists a wide variety of string types, produced with different materials and from different manufacturers. Core materials, winding methods, and construction technologies differ between string types, determining their unique acoustic properties. These are often labelled from string manufacturers with qualitative terms, such as "brilliant", "warm", "responsive". This work addresses the question: what are the differences in tone and playability of different string types.

In comparing string types, Norman Pickering made a significant contribution, systematically measuring tonal variations and transient time across numerous strings.[1–3] Pickering's results, detailed in his seminal work, include harmonic intensity graphs and the minimum bow force required to initiate a note.[1] His experiments revealed that strings with different core material, whether it is gut, synthetic, or metallic material, exhibit differences in brightness, frequency uniformity, and tonal quality.[4]

Pickering's experiments involved exciting the strings with a bowing machine that allow to vary the bow speed, bow force, and position along the string. More recent studies, such as those by Galluzzo[5] and Schoonderwaldt,[6,7] improved our understanding of playability and tonal quality of bowed strings by investigating in detail the role of bowing parameters. For example, Galluzzo built Schelleng diagrams with experimental data[8] and Schoonderwaldt overlaid spectral features onto Schelleng diagrams, creating what he called "sound palettes", that visually represent tonal features across bowing parameters.[7] These studies enabled the experimental identification of the playability range, but also the musicians' control strategies to manipulate the tone.

Schelleng diagrams with spectral features proved to be a valuable and informative tool to visualize and to provide a comprehensive view of playability and tonal quality. In this study, we adopt a similar experimental approach to investigate how cello string type influences tonal characteristics and playability. Using a robotic arm as bowing device and a custom monochord, we tested eight distinct G cello string types, each defined by a unique combination of core material, winding, and operating tension. We constructed high-resolution Schelleng diagrams to analyse playability differences and tonal variations across a wide range of bowing conditions. A total of 44 Schelleng diagrams were obtained, covering three different bow speeds, repeated measurements for the same strings, and multiple nominally identical strings to evaluate within-type variability. Additionally, two diagrams were recorded for the same string before and after extensive playing to assess settling effects.

While previous work has examined attack playability among different string types,[9] the focus in this work remains on the steady-state regime, analysing bow force limits, and spectral features such as pitch flattening, spectral centroid, and the presence of anomalous low frequencies. Furthermore, this study investigates possible trends about how the mechanical properties of strings, such as operating tension, bending stiffness, and damping, result in diverse acoustic responses.

2. METHODOLOGY

A. MEASUREMENTS

In this study, we collected recordings of bowed strings vibration to create Schelleng diagrams for different cello strings with a dedicated experimental setup. The experimental setup was designed to enable systematic measurements of bowed strings under controlled conditions. A robotic arm is embedded with a sensing bow used for bowing a single cello string mounted on rigid terminations and a standard guitar pick to measure the pluck response of the string. The robotic arm and the string are mounted on an optical table, minimizing external resonances and ensuring a stable environment for measuring string vibrations. A sensing bridge measures both static and dynamic bridge forces at one string termination, providing the data of the string vibration. Additional sensors at the nut measure string tension and the

nut force. Bow force was measured using two load cells installed on the bow, and bowing position and velocity were retrieved from the robotic arm position. Pluck responses were used to tune the string to its nominal frequency through an integrated self-tuning mechanism, and to estimate the mechanical properties of the string. Detailed descriptions of the setup and its prior applications can be found in a related technical report[10] and previous studies.[9, 11, 12]

We tested eight G2 cello string types, custom-made by D'Addario for these experiments. Each string was mounted on the setup without prior use and subjected to continuous bowing for approximately two hours (equivalent to around 3600 bow strokes) to stabilize its behaviour. During this settling period, the string was retuned to its nominal frequency every 200 strokes.

The Schelleng diagrams were generated by collecting the string vibration from the bridge sensor. The string was excited using a defined set of bowing parameters, consisting of 40 different positions along the string and 50 bow forces. Each combination of bowing parameter corresponds to a single stroke, resulting in 2000 strokes per diagram. For each point of the Schelleng diagram, the velocity is the same. Only the steady-state response of the string was considered, that is, when both bow force and velocity are constant.

The bow position along the string ranged from $1.4\,\mathrm{cm}$ to $14\,\mathrm{cm}$ from the bridge (corresponding to a relative bow-bridge distance $\beta = (0.02 - 0.2)$, logarithmically spaced, and bow force $F_\mathrm{b} = (0.1\,\mathrm{N} - 4\,\mathrm{N})$, logarithmically spaced. We used three bow speeds v_b ($0.05\,\mathrm{m\,s^{-1}}$, $0.1\,\mathrm{m\,s^{-1}}$, $0.2\,\mathrm{m\,s^{-1}}$). These values are consistent with ranges used by cello players[13] and previous similar studies involving bowing machines.[8]

Measurements were conducted within a region of the bow hair where F_b remained almost constant during the strokes. F_b was not directly controlled, as in PID systems, but solely from the elevation of the bow, wich was kept constant during the stroke. The measurements were carried out scanning the F_b–β parameter space, changing the bowing parameters in ascending order. At each change of β, the string was tuned to its nominal frequency, and six additional pluck responses were recorded. These responses were analysed to monitor string properties.

B.   STRING SAMPLES

For this study, eight string types with a unique set of material and nominal tension were tested. We used strings with four distinct core and outer winding materials. The string denoted as A has steel core and tungsten winding; string B has stranded steel core and tungsten/silver winding; string C has nylon core and silver winding; string D has steel core and nickel winding. Each type was manufactured with a lower and higher nominal tension, denoted by T1 and T2, respectively. A key implication of varying tensions is that the geometry of the strings had to be altered to maintain consistent material properties across the different tension variants.

The mechanical properties were estimated from the string pluck responses collected over the course of the the Schelleng diagram measurements. The fundamental frequency f_0, linear density μ, the transverse impedance Z, damping factors ζ and the bending stiffness EI were computed. The tension T was measured with a dedicated sensor at the nut. Values of these mechanical properties are shown in Tab. 1 with their average and standard deviation across the plucks, except the diameter and the torsional stiffness that were provided from the manufacturer. Fig. 1 shows the damping factors as a function of the mode number. Modes in which the damping factors weren't estimated accurately from the experimental fit were discarded.

The mechanical properties across the eight strings show little difference. Within the ones with unique material compositions (A, B, C, and D) the parameters show a variation of about 13% (mean absolute percentage difference) and of about 15% between the two tension groups (T1 and T2). Specifically, the bending stiffness of the group T2 is 32% larger than the one of T1. The torsional stiffness is around 15% smaller for group T2. Similar differences were observed across the strings with unique material compositions. Regarding the damping factors, a comparison among common vibrational modes show that the difference between strings with unique materials is more pronounced than the difference between T1 and T2, around 30% versus 20%, respectively. This suggests that material and design play a more significant role in damping than changing the nominal tension. However, not all the modes exhibit the

same level of variation. Some modes, like mode 4 and 9, show the largest differences across different string with unique materials (50%-60%). Mode 1, on the contrary, exhibits a higher level of variation between tension groups (27% versus 17%).

Group	String	d† (mm)	T (N)	μ (g/m)	Z (kg/s)	Z_{to}† (gm^2/s^2)	EI (10^{-4}Nm^2)
T1	A	0.947	145.31 ± 0.23	7.721 ± 0.007	1.0592 ± 0.0011	0.039	3.032 ± 0.115
	B	0.927	150.87 ± 0.31	8.017 ± 0.010	1.0998 ± 0.0015	0.055	4.397 ± 0.166
	C	1.077	144.40 ± 0.30	7.671 ± 0.013	1.0525 ± 0.0018	0.039	3.142 ± 0.182
	D	1.123	142.67 ± 0.29	7.578 ± 0.011	1.0398 ± 0.0016	0.064	5.246 ± 0.212
T2	A	1.001	163.03 ± 0.75	8.662 ± 0.012	1.1884 ± 0.0028	0.027	3.969 ± 0.156
	B	0.973	163.23 ± 0.78	8.674 ± 0.011	1.1899 ± 0.0030	0.060	7.295 ± 0.588
	C	1.083	153.04 ± 14.04	8.128 ± 0.745	1.1154 ± 0.1023	0.040	3.969 ± 0.398
	D	1.201	164.82 ± 1.30	8.767 ± 0.014	1.2021 ± 0.0045	0.039	5.766 ± 0.466

Table 1: String properties the cello strings used for this study. They are grouped according to their unique material composition (A-D) and their nominal tension (T1 and T2). † Values for d and Z_{to} were provided by the string manufacturer and are presented without standard deviation.
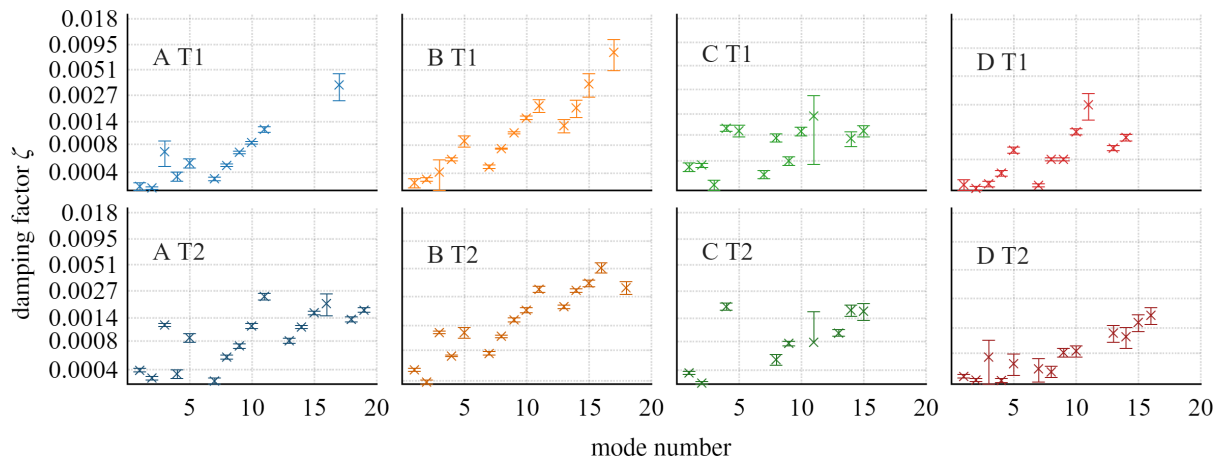

Figure 1: Damping factor ζ of the T1 and T2 cello strings (values in logarithmic scale). Average values and high and low intervals over the plcuks are shown.

3. SCHELLENG DIAGRAMS

The vibration regimes were determined from the bridge force signals using an algorithm for automated identification based on a previous work.[5] Fig. 2b shows the bridge force signals corresponding to the vibration regimes. The vibration regimes are plotted as a function of F_b and β in Fig. 2a, where the Schelleng diagrams for three bow speeds are presented. The vibration regime locations in the Schelleng diagrams correspond to qualitatively similar patterns found in earlier experimental studies.[6,8]

The Helmholtz motion is considered the vibration regime that corresponds to the standard sound produced by a bowed string instrument. For this reason, the area populated mostly by this regime delineates the playable region. Below this region, the string tends to vibrate with two slips per period, and also more if the bow force is particularly low. Above the playable region, on the contrary, the string exhibits mostly raucous motion and S-motion regimes of vibration. Multiple fly-back motion instances were identified, especially within and above the playable region. When increasing the bow speed, the playable region moves to higher bow forces, as expected from the literature[14] and previous experiments.[6]
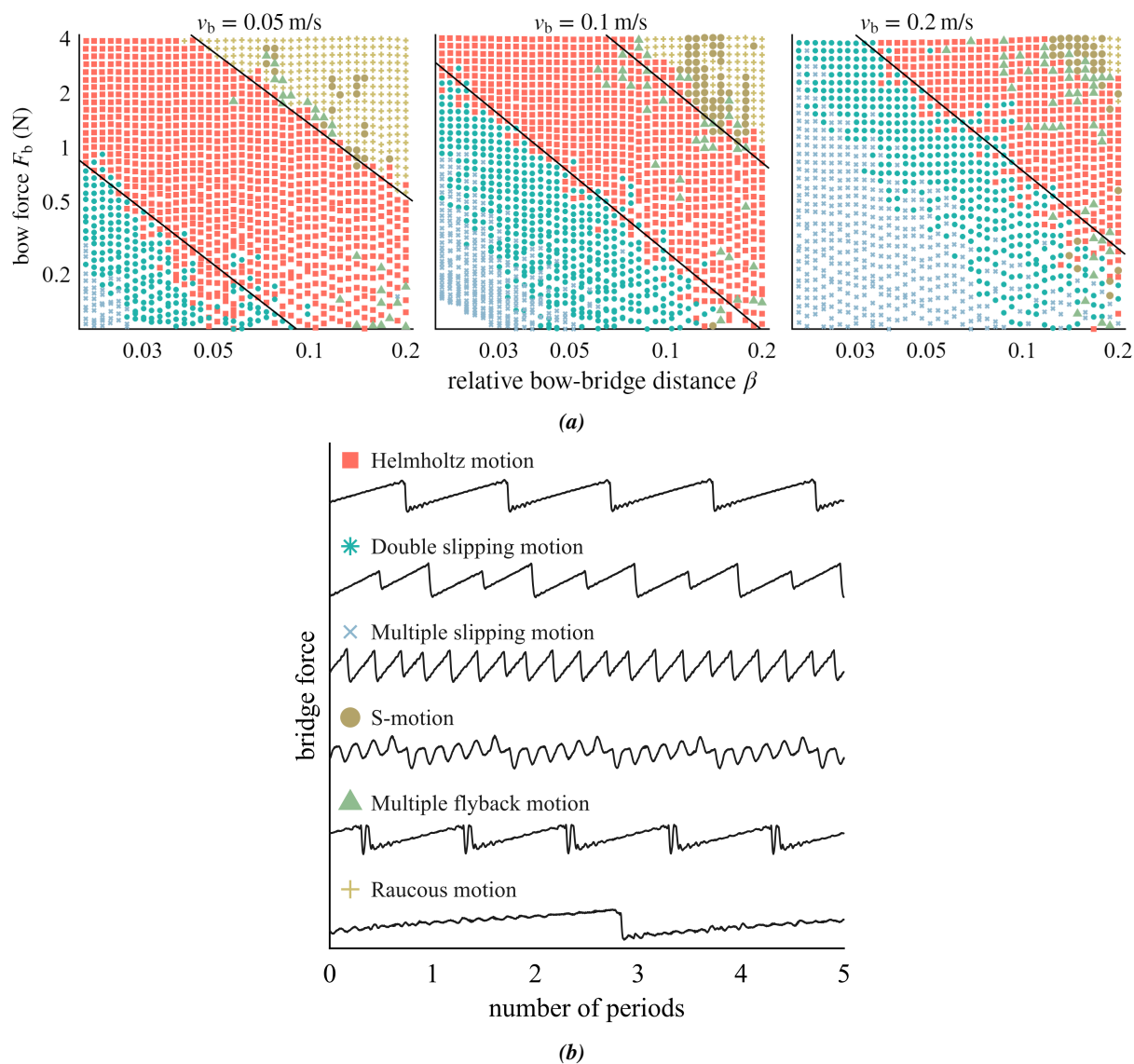
(a)

(b)

Figure 2: (a): Example of the experimental Schelleng diagrams and the bow force limits for three bow speeds. The vibration regimes are labelled with the same markers as in (b). The string used in this example is A T1. (b): Bridge force signals corresponding to the different vibration regimes.

A. BOW FORCE LIMITS

According to the Schelleng's theoretical formulation,[15] the playable region is delimited by an upper limit and lower limit of the bow force, that are, the maximum and minimum bow force to produce Helmholtz motion. The lower limit is proportional to v_b/β^2, while the upper limit to v_b/β. These proportionalities were found to be inaccurate in light of experimental measurements[6, 16] and comprehensive models of the bow-string interaction.[17] For this reason, we identified the upper and lower limits by fitting a generic function $F_b = c\beta^\alpha$ to the experimental borders of the playable region. The best-fit values of c and α were found to deviate from the theoretical prediction of Schelleng, confirming the previous findings. The experimental borders were identified by the points where at least three consecutive data points with Helmholtz motion were present along one column of β. This excludes the points that belong to regions where the Helmholtz motion is not clearly present, like in the "patchy Helmholtz" area[8] or near S-motions. For the highest speed of $0.2\,\mathrm{m\,s^{-1}}$ the upper limit was not computed because the borders were not clearly identifiable as they approached the maximum bow force used in these measurements. The fitted limits are drawn in the Schelleng diagrams of Fig. 2a with solid black lines.

B. PITCH FLATTENING

For the cases of Helmholtz motion, the pitch is computed to investigate the pitch flattening effect, that is, when the pitch drops due to a particularly high bow force.[18] The deviation of the pitch to the nominal 98 Hz is displayed in Fig. 3. The pitch flattening mostly appears in the top-right region of each playable region, close to the upper bow force limit. On average, we observed pitch deviations of around -6 cents, but under certain conditions, deviations reached -50 or even -60 cents, corresponding to roughly 96-95 Hz. Overall, flattening tends to be more pronounced at lower bow speeds, while pitch rises — that is, positive deviations — tend to occur at higher speeds. These results are in line with previous experimental findings[7] and also match numerical simulations.[19]
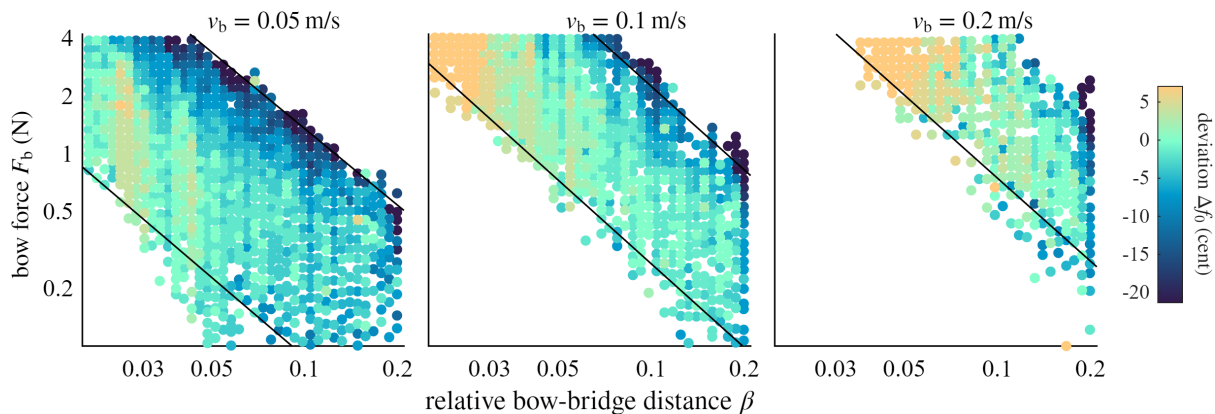

Figure 3: Pitch flattening for the Helmholtz motion cases of Fig. 2a.

C. SPECTRAL CENTROID

We computed the spectral centroid SC for the Helmholtz motion cases to map the "brightness" of the sound across the Schelleng diagram, as suggested by Schoonderwaldt.[7] We limited the upper frequency of the spectral centroid computation to $1.5\,\mathrm{kHz}$ to filter out noise, especially since it becomes more dominant at low bow forces. The spectral centroid profiles showed a nonlinear trend as a function of F_b and β, as illustrated in Fig. 4. In some cases, we observed the spectral centroid increasing at particular values of β. This might be due to β being close to a node of the string's vibration, affecting the harmonic content. Overall, the centroid tends to increase with bow force, as expected.
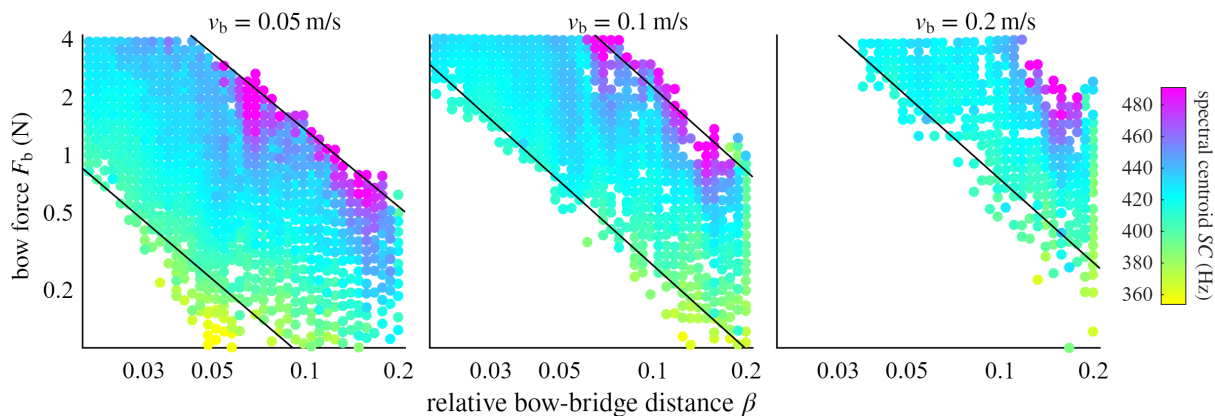
Figure 4: Spectral centroid for the Helmholtz motion cases of Fig. 2a.

D.   ANOMALOUS LOW FREQUENCIES

In some cases, the string can be forced to vibrate with much lower fundamental frequencies than f_0, called anomalous low frequencies (ALFs).[20] They can reach one or more harmonics below f_0. This behaviour has been reported in experiments using violin strings,[7] where higher bow forces are needed to trigger ALFs. No cases were previously reported in the literature for cello string experiments.

In our Schelleng diagrams, we found ALFs by looking for periodic signals with a frequency lower than 80 Hz, that is around three semitones below the natural frequency f_0. We included signals from 12 additional Schelleng diagrams where the highest F_b was about 12 N (not discussed in this paper). All the instances of ALFs we found are collected in Fig. 5. At $v_b = 0.05\,\mathrm{m\,s}^{-1}$, ALF cases tend to cluster along a line in the diagram. For low F_b values, a very large β is required for ALFs to occur. As one moves the bow closer to the bridge, a higher bow force is required to trigger ALFs. Most of the ALF occurrences happen above 4 N — up to 16 N in some cases. However, for strokes at $0.1\,\mathrm{m\,s}^{-1}$, we don't have enough data to clearly identify this trend. Furthermore, we did not observe ALFs at $0.2\,\mathrm{m\,s}^{-1}$, which suggests that ALFs emerge primarily at low bow speeds and high bow forces, consistent with earlier experimental data.[7] In terms of frequency, the ALFs we found are shown in Fig. 5. Most of them are in the range of 45 Hz, which is close to the first subharmonic of the fundamental. In some cases, the fundamental drops to a few octaves below the nominal pitch, reaching around 27 Hz, especially in the very top region of the Schelleng diagram at $0.05\,\mathrm{m\,s}^{-1}$.
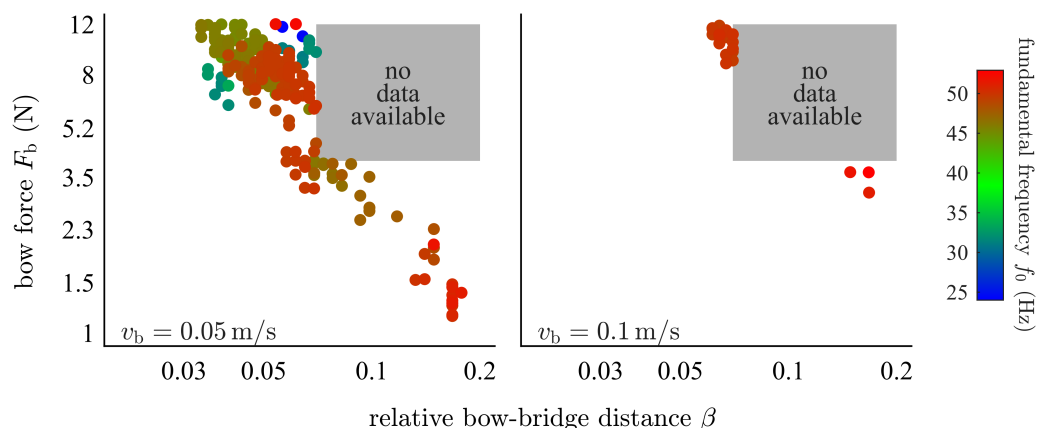

Figure 5: ALFs instances found in all the Schelleng diagrams. Data from measurements with a high bow force (up to 12 N) are included.

4. STRINGS COMPARISON

Generally, these abovementioned trends of the bow force limits, pitch flattening, spectral centroid and ALFs agree with previous findings, and they are consistent across all strings we tested. On the other hand, differences across the strings can be found by visually inspecting all the Schelleng diagrams or by extracting high level features that would represent the main aspects of each string's playability, brightness, and tendency to pitch flattening. We extracted significant features from each Schelleng diagram to capture the general trend across bowing parameters.

To highlight the role of material and tension separately, the strings sharing the same material composition were grouped and compared to each other, while the tension group T1 was compared with the tension group T2. This comparison was carried out by computing the absolute difference of the features for each group and for each bow speed.

To assess whether the observed differences in these features arose from systematic errors in the setup, procedure or analysis, we computed the variation of the features between two additional Schelleng diagrams that were obtained by consecutive measurements. Since the string used for these diagrams (B T2) was played for a long time before to stabilize its vibrational behaviour, we can consider these measurements as repetitions of the same string and use the features difference as a baseline. In this paper, we will present only the comparisons that are associated with a difference significantly exceeding the baseline.

Regarding playability, we computed the playability area A_p — that is, the area enclosed between the upper and lower bow force limits derived from exponential fits. The resulting playability areas are shown in Fig. 6. The biggest difference of A_p at $v_b = 0.05\,\mathrm{m\,s^{-1}}$ was found between strings B and C, with an absolute difference of 0.04, while the absolute difference of the baseline (the consecutive repetitions) was of 0.004; at $v_b = 0.1\,\mathrm{m\,s^{-1}}$ the highest difference was found between A and B (0.054) but it was below the baseline (0.056); at $v_b = 0.2\,\mathrm{m\,s^{-1}}$ between C and D we found a difference of 0.042 with a baseline 0.0032. It was also observed that the playability area differences between operating tension (strings of T1 group versus T2 group) were of the same order as the ones between materials: at $v_b = 0.05\,\mathrm{m\,s^{-1}}$ it was of 0.0214; at $v_b = 0.1\,\mathrm{m\,s^{-1}}$ was 0.0048 and at $v_b = 0.2\,\mathrm{m\,s^{-1}}$ was 0.0075. The differences across materials were found to be sometimes smaller than the ones between tension groups or the baseline, and no clear trend was peaking out.
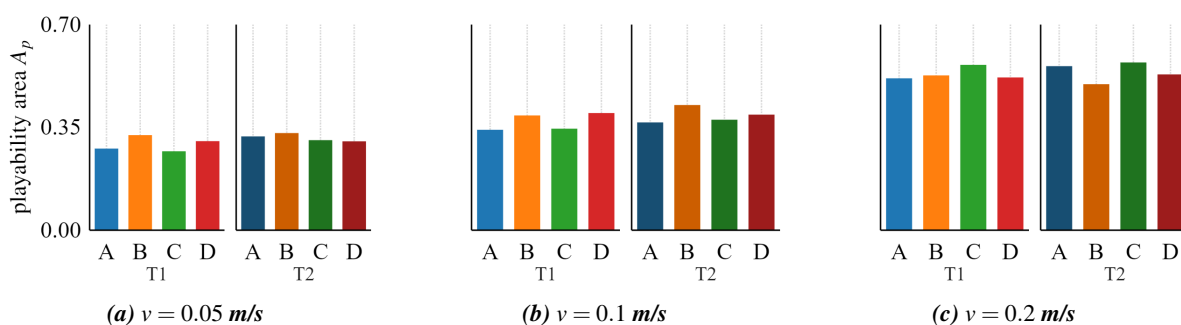

Figure 6: Comparison of the playability areas across strings and bow speeds extracted from the Schelleng diagrams.

In Fig. 7, the features extracted from the pitch deviation of the Schelleng diagrams are shown: the box plots show the upper bound of pitch deviation — defined as the average of the 95th percentile of pitch deviation values within each Schelleng diagram — and the the lower bound, defined as the average of the 5th percentile of the data, and the averaged value represented by a white mark. For the comparison, we consider only the 5th percentile, as it shows the lowest pitch deviation from each case. The trend of this feature is not consistent among bow speeds, except for string B that tends to have the highest value among other strings. At $0.05\,\mathrm{m\,s^{-1}}$, it is clear that the biggest difference is between string C and B (10.7 cents with a baseline of 0.4 cents); similarly, at $0.1\,\mathrm{m\,s^{-1}}$, the most substantial differences were observed between string B and C (19 cents with a baseline of 5 cents), while at $0.2\,\mathrm{m\,s^{-1}}$, between string C and D

(8.9 cents with a baseline of 2.8 cents). The difference between T1 and T2 was around 5 cents at each speed.

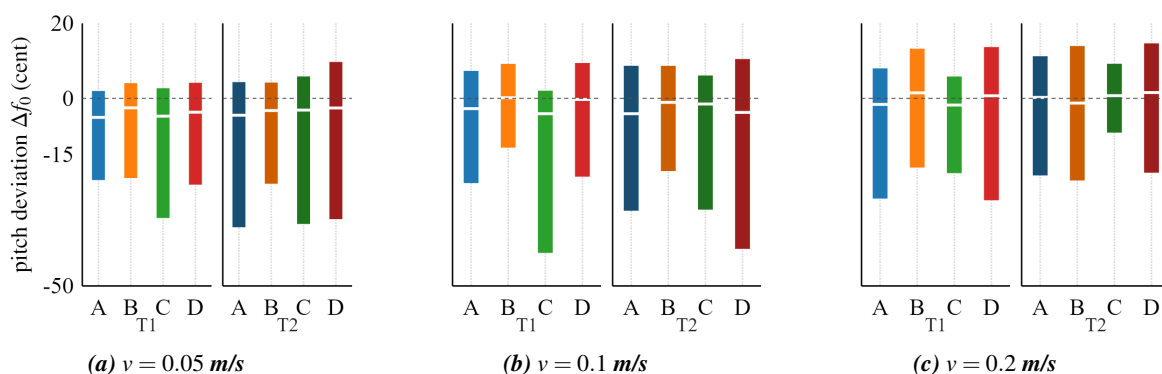*(a) $v = 0.05$ m/s*   *(b) $v = 0.1$ m/s*   *(c) $v = 0.2$ m/s*

Figure 7: Comparison of the pitch deviation across strings and bow speeds extracted from the Schelleng diagrams.

Fig. 8 shows the spectral centroid, including the mean, as well as the 5th and 95th percentiles, computed for each Schelleng diagram. The comparison takes into consideration only the mean. We observe a trend that is more consistent across bow speeds and tension groups than in the previous comparisons. The highest differences have to be attributed to string A and B and to string B and C. The average *SC* of string A is consistently higher than the one of string B. Similarly, the *SC* of string B is lower than the one of string C for all the bow speeds. This trend is minimal at $v_b = 0.2 \, \mathrm{m \, s^{-1}}$ for the T2 group. Finally, also string B shows a slightly lower *SC* than string D for all the cases. These trends of the spectral centroid may indicate a potential relationship with material properties.

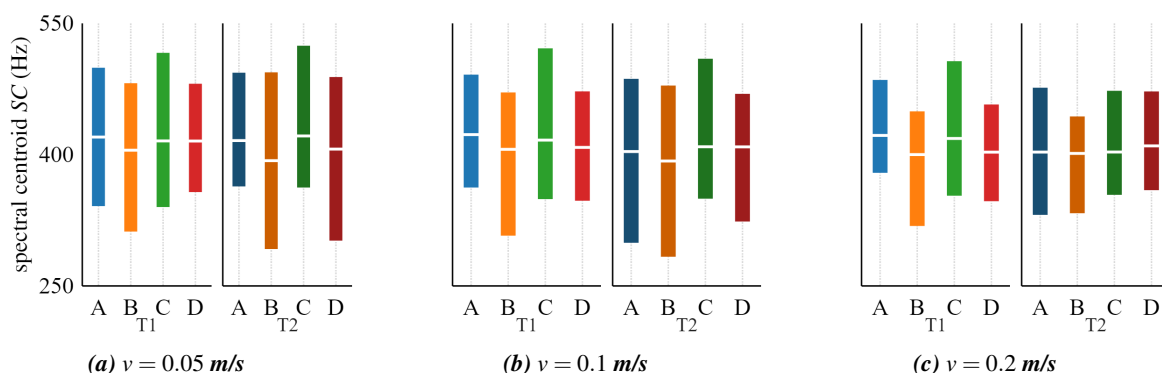*(a) $v = 0.05$ m/s*   *(b) $v = 0.1$ m/s*   *(c) $v = 0.2$ m/s*

Figure 8: Comparison of the spectral centroid across strings and bow speeds extracted from the Schelleng diagrams.

We compared the average spectral centroid with the bending stiffness because it gives a good picture of the material composition. This helped us learn more about the possible effect of string property on the spectral centroid. We found an overall trend: as bending stiffness increases, the spectral centroid decreases. This can be observed in Fig. 9, where the average spectral centroid values are plotted against the bending stiffness of the string tested.

Although additional correlations between playability, pitch flattening, spectral centroid and other material properties (e.g., damping factors) were explored, they don't show consistency across bow speeds, and therefore do not allow for strong conclusions regarding the material properties influence at this stage.

We also tested three additional samples of the string labeled A T1. The differences in mechanical properties observed across these samples were significantly smaller than those observed across different material or tension groups. This low variability was partially reflected in the extracted acoustic features
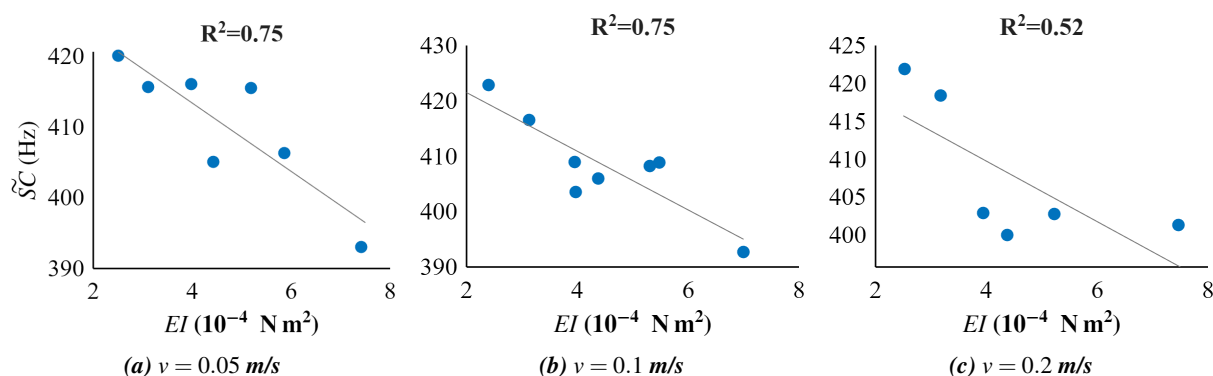
Figure 9: *Correlation between the averaged spectral centroid and the bending stiffness for different strings across bow speeds.*

as well: the spectral centroid, playability area, and pitch flattening features that were discussed for the comparisons all showed only minimal differences comparable to the baselines.

An additional test involved recording Schelleng diagrams (only at $0.1\,\text{m s}^{-1}$) and extracting the features at different stages of the string's lifetime, specifically, immediately after mounting for the first time, and after a longer playing session involving several thousand bow strokes. In this case, the differences across features were minimal regarding the playability area, but significant for the flattening and spectral centroid, comparable to the ones between material compositions. This highlights the importance of the settling period of the string, and how playing the string changes its tone.

5.   DISCUSSION AND CONCLUSIONS

This study provides an experimental assessment of how different cello string types influence playability and tonal characteristics, employing Schelleng diagrams with spectral features. The use of a robotic bowing device and a custom monochord setup allowed for controlled and repeatable excitation conditions, isolating the influence of string properties from performer-related variability.

The results confirm and extend previous findings on the relationship between bowing parameters and the regimes of string vibration. Helmholtz motion was observed to dominate within bounded regions of the Schelleng diagrams, consistent with classical theory and previous empirical work. The dependence of bow force limits on β and v_b was found to deviate from Schelleng's original relationships, in agreement with more recent studies that suggest refinements to these formulations.[6, 16]

Pitch flattening emerged mostly at high bow forces and low speeds, with deviations of up to 60 cents below the nominal pitch. Interestingly, the degree of flattening did not correlate consistently with material composition, but rather appeared more sensitive to bow speed. Spectral centroid analysis revealed more systematic trends. Strings with higher bending stiffness tended to exhibit lower average spectral centroids, suggesting a perceptually less "bright" tone. This trend was observed consistently across bow speeds and appears to reflect an underlying material dependency. Anomalous low frequencies (ALFs), previously reported primarily in violin strings, were also observed under extreme bowing conditions on cello strings. These regimes emerged predominantly at low bow speeds and high forces.

Importantly, within-type variability—assessed through repeated measurements of nominally identical strings—was found to be minimal, both in terms of mechanical and acoustic features. However, tonal changes due to string settling were non-negligible, particularly for spectral centroid and pitch flattening. These observations highlight the importance of string "play-in" time.

Overall, while playability areas were found to vary between some string types, they remained relatively stable across tension groups. Tonal descriptors, particularly spectral centroid, proved more sensitive to material differences than to tension variation. This suggests that core and winding materials exert a greater influence on tonal brightness than nominal string tension, at least within the bowing parameters range and samples tested.

It is important to emphasise that the findings presented here reflect observable trends rather than definitive statistical conclusions, due to the limited number of string samples tested. Future research should therefore prioritise the collection of data from a broader range of strings to improve statistical robustness. Introducing greater variability—for instance, by including strings of different pitches and from various musical instruments—would help to generalise the results and support more conclusive interpretations. In particular, we recommend focusing on spectral features, especially those associated with perceived brightness, as this study revealed a promising correlation with material properties. A more detailed examination of individual harmonic content may also uncover subtle nuances in string timbre.

Data Availability Statement: Data relevant to the study (for example, raw and processed recordings) are available at https://iwk.mdw.ac.at/projects/fwf-the-bowed-string/

AUTHOR CONTRIBUTIONS

Conceptualization and design of the analysis, A.L, and V.C; project administration, and supervision, V.C.; investigation, software, data collection and curation, and visualization, A.L.; writing—original draft, A.L.; writing—review and editing, A.L, V.C. and G.S.; funding acquisition, V.C.. All authors have read and agreed to the published version of the manuscript.

ACKNOWLEDGMENTS

REFERENCES

[1] Norman Pickering. *The Bowed String: Observations on the Design, Manufacture, Testing and Performance of Strings for Violins, Violas and Cellos.* Amereon, 1991.

[2] Norman Pickering. Material considerations in musical strings. *MRS Bulletin*, 20(3):32–33, 1995.

[3] Norman C. Pickering. Physical properties of violin strings. *Catgut Acoustical Society Journal (CAS Journal)*, (44):40031, 1985.

[4] Norman Pickering. String tone quality related to core material. *Catgut Acoustical Society Journal*, 1(5):23–28, 1990.

[5] Paul Galluzzo. *On the playability of stringed instruments*. PhD thesis, University of Cambridge, 2004.

[6] Erwin Schoonderwaldt, Knut Guettler, and Anders Askenfelt. An empirical investigation of bow-force limits in the schelleng diagram. *Acta Acustica united with Acustica*, 94(4):604–622, 2008.

[7] Erwin Schoonderwaldt. The violinist's sound palette: spectral centroid, pitch flattening and anomalous low frequencies. *Acta Acustica united with acustica*, 95(5):901–914, 2009.

[8] Paul Galluzzo and Jim Woodhouse. High-performance bowing machine tests of bowed-string transients. *Acta Acustica united with Acustica*, 100(1):139–153, 2014.

[9] Alessio Lampis, Alexander Mayer, and Vasileios Chatziioannou. An experimental approach for comparing the influence of cello string type on bowed attack response. *JASA Express Letters*, 4(11), 2024.

[10] Alexander Mayer and Alessio Lampis. A versatile monochord setup: An industrial robotic arm as bowing and plucking device. Technical report, Department of Music Acoustics - Wiener Klangstil (IWK), 2024. https://doi.org/10.21939/iwk-tech-report-1-2024.

23 September 2025 12:58:28

[11] Alessio Lampis, Alexander Mayer, Montserrat Pàmies-Vilà, and Vasileios Chatziioannou. Examination of the static and dynamic forces at the termination of a bowed string. *The Journal of the Acoustical Society of America*, 153(3_supplement):A198–A198, 2023.

[12] Alessio Lampis, Alexander Mayer, and Vasileios Chatziioannou. Assessing playability limits of bowed-string transients using experimental measurements. *Acta Acustica*, 2024. accepted for publication.

[13] Timothy Wofford. *Study of the interaction between the musician and the instrument. Application to the playability of the cello*. PhD thesis, Sorbonne université, 2018.

[14] John Schelleng. The physics of the bowed string. *Scientific American*, 230(1):87–95, 1974.

[15] John Schelleng. The bowed string and the player. *The Journal of the Acoustical Society of America*, 53(1):26–41, 1973.

[16] Robert Mores. Maximum bow force revisited. *The Journal of the Acoustical Society of America*, 140(2):1162–1171, 2016.

[17] Hossein Mansour, Jim Woodhouse, and Gary P Scavone. On minimum bow force for bowed strings. *Acta Acustica united with Acustica*, 103(2):317–330, 2017.

[18] Xavier Boutillon. Analytical investigation of the flattening effect: the reactive power balance rule. *The Journal of the Acoustical Society of America*, 90(2):754–763, 1991.

[19] Hossein Mansour. *The bowed string and its playability: Theory, simulation and analysis*. PhD thesis, McGill University, 2016.

[20] Knut Guettler. Wave analysis of a string bowed to anomalous low frequencies. *Catgut Acoust. Soc. J*, 2(6):8–14, 1994.

23 September 2025 12:58:28